Geomechanics and Engineering, *Vol. 33, No. 1 (2023) 11-18*
https://doi.org/10.12989/gae.2023.33.1.011

New energy partitioning method in essential work of fracture (EWF) concept for 3-D printed pristine/recycled HDPE blends

Sukjoon Na[1a], Ahmet Oruc[1b], Claire Fulks[1c], Travis Adams[1d], Dal Hyung Kim[3e], Sanghoon Lee[2f] and Sungmin Youn[*1]

[1]*Department of Civil Engineering, Marshall University, One John Marshall Drive, Huntington, WV 25755, USA*
[2]*Department of Computer Sciences and Electrical Engineering, Marshall University, One John Marshall Drive, Huntington, WV 25755, USA*
[3]*Department of Mechanical Engineering, Kennesaw State University, 1000 Chastain Road, Kennesaw, GA 30144, USA*

(*Received November 10, 2022, Revised January 31, 2023, Accepted February 8, 2023*)

Abstract. This study explores a new energy partitioning approach to determine the fracture toughness of 3-D printed pristine/recycled high density polyethylene (HDPE) blends employing the essential work of fracture (EWF) concept. The traditional EWF approach conducts a uniaxial tensile test with double-edge notched tensile (DENT) specimens and measures the total energy defined by the area under a load-displacement curve until failure. The approach assumes that the entire total energy contributes to the fracture process only. This assumption is generally true for extruded polymers that fracture occurs in a material body. In contrast to the traditional extrusion manufacturing process, the current 3-D printing technique employs fused deposition modeling (FDM) that produces layer-by-layer structured specimens. This type of specimen tends to include separation energy even after the complete failure of specimens when the fracture test is conducted. The separation is not relevant to the fracture process, and the raw experimental data are likely to possess random variation or noise during fracture testing. Therefore, the current EWF approach may not be suitable for the fracture characterization of 3-D printed specimens. This paper proposed a new energy partitioning approach to exclude the irrelevant energy of the specimens caused by their intrinsic structural issues. The approach determined the energy partitioning location based on experimental data and observations. Results prove that the new approach provided more consistent results with a higher coefficient of correlation.

Keywords: 3D printing; energy partitioning method; essential work of fracture (EWF); fracture toughness; fused deposition modeling (FDM); high-density polyethylene (HDPE); recycled plastics

1. Introduction

Throughout the past few decades, the use of polymeric materials in civil and environmental engineering projects has steadily increased. With good mechanical properties and chemical resistance, high-density polyethylene (HDPE) has been particularly demanded in the construction of infrastructures such as geosynthetic-reinforced retaining walls, pavements, landfills, and pipeline networks as well as household products (Terzi *et al.* 2015, Liu *et al.* 2017). According to American Chemistry Council (ACC) (American Chemistry Council 2022), the total production of major plastic resins in the U.S. including polyethylene (PE), polypropylene (PP), polystyrene (PS), polyvinyl chloride (PVC), and others reached more than 106 billion pounds in 2021, which was increased by approximately 40% from 2011. 49% of the total production came from PE, and HDPE made up 42% of PE (Fig. 1).

In general, polymeric materials including HDPE come from petroleum supplies. Furthermore, a significant increase in the use of plastics has promoted concerns regarding accumulated plastic waste in the environment. Therefore, plastics are not an ideal material in terms of environmental sustainability. To improve the sustainability of plastics, utilizing post-consumed plastics has been strongly considered and encouraged in various engineering fields including geotechnical engineering. For example, Usman *et al.* (2021) studied the applicability of irradiated waste polyethylene terephthalate in asphalt pavement as fine aggregate substitutes. Ghadr *et al.* (2019) tested expansive soils blended with a waste tyre sand-sized rubber (a mixture of polybutadiene, polyisoprene, elastomers, and styrene-butadiene) and found that the inclusion of those waste materials substantially decreased the swelling potential/pressure and lowered the compression index of expansive soils.

However, recycled plastics tend to have limited mechanical properties compared to their pristine counterpart. The recycling process can cause changes in the microstructure and mechanical properties of the polymer due to high temperature and intensive shearing. This process leads to the thermal and mechanical degradation of polymers. Aurrekoetxea *et al.* (2001) observed that the melt

*Corresponding author, Assistant Professor
E-mail: youns@marshall.edu
[a]Ph.D.
[b]Graduate Student
[c]Undergraduate Student
[d]Undergraduate Student
[e]Ph.D.
[f]Ph.D.

ISSN: 2005-307X (Print), 2092-6219 (Online)

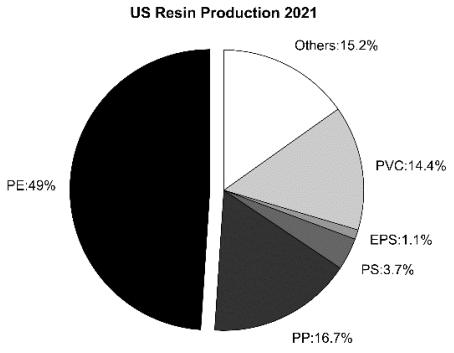

Fig. 1 US plastic resin production in 2021

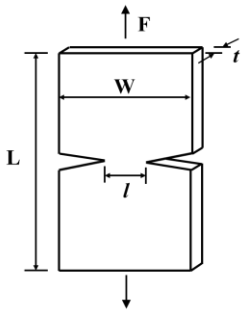

Fig. 2 Geometry of DENT specimen

flow index (MI) of isotactic polypropylene (iPP) increased after a certain number of recycling cycles. This result reflects the reduction of molecular weight and the increase in the degree of crystallinity of the polymer due to the recycling process. The degree of crystallinity is highly correlated with mechanical properties such as elastic modulus and yield stress. In addition, the flexibility of a polymer is dependent on the mobility of polymer chains, which is prevented by crystalline structures. As a result, a polymer with high crystallinity tends to have a higher modulus or stiffer. Similar effects of reprocessing process on various polymers have been reported in many experimental studies. For example, (Pattanakul *et al.* 1991, La Mantia 1999) reported that reprocessing of HDPE made the material more brittle and decreased the elongation at break significantly. (Na *et al.* 2015, Na *et al.* 2016, Na *et al.* 2016, Na *et al.* 2018) also found that blending recycled HDPE with pristine HDPE decreased the number and size of fibrils that are connecting new fracture surfaces. The reduction of fibrils lowered the fracture toughness and reduced the stress crack resistance of HDPE, resulting in earlier failure than its pristine one. Therefore, many studies have attempted to compensate for a loss of properties of recycled HDPE or enhance targeted properties to promote the use of recycled polymers in engineering applications.

Fracture toughness is one of the key parameters in engineering applications. It indicates the ability of a material to resist cracking or fracturing. In geotechnical engineering, the parameter is often used to measure the crack resistance of rock and cemented paste backfill mixes (Komurlu *et al.* 2016, Maruvanchery and Kim 2019). Fracture toughness is determined by measuring the energy required to create new crack surfaces in a material body. Although most laboratory fracture tests are now well-developed and standardized, they still require a tedious and time-consuming process, particularly for the preparation of test specimens. For example, one of the most popular fracture testing, the *J*-integral test, requires complex specimen geometries such as compact-tension (CT) specimens with an accurate size of the pre-determined crack. Although some other fracture tests such as the essential work of fracture (EWF) concept have less rigorous specimen geometry requirements (Wu and Mai 1996, Ching *et al.* 2000), they still require precisely manufactured specimens. The EWF test uses a double-edge notched tension (DENT) specimen which includes initial straight notches in a specimen, as shown in Fig. 2. and the shape and sharpness of a notch tip significantly affect the quality of specimens. Therefore, manufacturing multiple specimens that have the identical geometry of a notch-tip is the top priority of the EWF test.

Recently, additive 3D printing techniques have revolutionized the manufacturing process involving various polymers, metals, and even concrete. Extrusion-based 3D printing such as the fused deposition modeling (FDM) technique uses polymer filaments fed into a heated nozzle and extrudes polymer melt to a print bed to build a 3D product layer-by-layer. Because 3D printing enables the fabrication of complex structures at a faster speed without any additional cost associated with traditional manufacturing setups such as industrial-size extruders and specimen molds, it has gained great attention not only in manufacturing industries but also in research that requires rapid prototyping of test samples. For successful fabrication in 3D printing, adhesion between a deposited polymer and a print bed is critical for the quality of a printed product. Amorphous polymers such as acrylonitrile-butadiene-styrene copolymers (ABS) or semi-crystalline polymers with low crystallinity such as polylactic acid (PLA) have good adhesion; therefore, they are commonly used in 3D printing. On the other hand, HDPE which has very high crystallinity has been problematic due to its poor adhesion, shrinkage, and warpage during the 3D printing process (Gudadhe *et al.* 2019, Schirmeister *et al.* 2019).

This paper suggests the optimized parameters and printing conditions found through parametric studies for the use of recycled HDPE blends in 3D printing. In addition, this paper discussed the potential problems of test specimens manufactured by the FDM 3D printing technique, particularly for the EWF test. Finally, the paper proposed a new energy partitioning method that overcomes the problems caused by the intrinsic structure of 3D printed models and measures fracture properties.

2. Review of EWF concept

The EWF concept has quickly become one of the most popular approaches to characterizing the fracture properties of ductile polymers due to its relatively simple test protocols and specimen preparation. It uses double-edge

notched tensile (DENT) type specimens with various ligament lengths and measures load-displacement response until the specimen completely fails (Fig. 2). The EWF concept was first proposed by Broberg (Broberg 1968; Broberg 1971, Broberg 1975) and elaborated by many other researchers for different materials and experimental conditions (Cotterell and Reddel 1977, Mai and Pilko 1979, Mai and Cotterell 1986). The concept is based on the assumption that the total work energy of the DENT specimen can be partitioned into two components: the surface energy and volumetric energy contributing to the formation and propagation of the crack. The surface energy refers to the energy consumed in the fracture process zone, while the volumetric energy relates to the plastic work in the outer process zone (OPZ). Therefore, the total work of fracture (W_F) can be written as the sum of essential fracture work (W_E) and non-essential plastic work (W_P)

$$W_F = W_E + W_P = w_e tl + \beta w_p tl^2 \quad (1)$$

where t and l are the thickness and ligament length of the DENT specimen, respectively. Normalizing Eq. (1) by the initial ligament area (tl) results in a linear equation about ligament length

$$w_f = w_e + \beta w_p l \quad (2)$$

where w_e is the specific EWF, w_p is the specific non-essential fracture work per unit volume, and β is the geometrical shape factor associated with OPZ. In Eq. (2), w_e equals w_f at zero ligament length; therefore, it becomes independent of specimen geometry (*i.e.,* ligament) and is considered a material constant. Mai and Cotterell (Mai and Cotterell 1986) demonstrated the theoretical equivalence between the specific EWF value and J_c, which is the fracture toughness of a material, as exhibited in Eq. (3).

$$w_f = J_c + \frac{dJ}{da}\frac{l}{4} \quad (3)$$

where J_c is the critical J value and a is a crack extension. This theoretical equivalence was experimentally verified by other studies (Mai and Cotterell 1986, Paton and Hashemi 1992, Wu *et al.* 1993, Levita *et al.* 1994, Wu and Mai 1996).

The EWF test protocol requires specific geometry of the test specimen, particularly the ligament length (Mai *et al.* 1987, Chan and Williams 1994, Williams and Rink 2007). For the upper limit, the entire ligament must yield fully prior to crack initiation. To achieve this condition, the initial ligament length must be less than the plastic zone size (r_p) ahead of the crack-tip. r_p is determined as

$$r_p = \frac{1}{2\pi}\left(\frac{Ew_e}{\sigma_y^2}\right) \quad (4)$$

where E is the elastic modulus, and σ_y is the material's yield stress. Additionally, the ligament length must be less than $W/3$ to prevent the edge effect caused by the limited size of the width. For the lower limit, the test should be conducted under the plane-stress condition. To fulfill the requirement, the ligament length should be three to five times greater than the thickness of the specimen. By considering the upper and lower limits together, the ligament length of DENT specimens should meet the size criterion which is written below

$$(3-5)t \le l \le min\left(\frac{W}{3}, 2r_p\right) \quad (5)$$

Table 1 Extrusion parameters for test materials

Parameters	Value
T_1 (nozzle)	190°C
T_2	195°C
T_3	200°C
T_4	205°C
Rotation speed	2 to 2.7 RPM

3. Materials and methods

3.1 Material preparation

Commercially available pristine HDPE resin (HDP0353, Braskem America) with a density of 0.947-0.955 g/cm^3 and melt index (MI) of 0.230 g/10 min was provided by Braskem America. Post-consumer recycled HDPE resin with a density of 0.961 g/cm^3, and MI of 0.642 g/10 min collected from number "2" stamped products such as milk jugs and water bottles were provided by Envision Plastics. These raw materials were provided in the form of pellets. The pristine and recycled HDPE blends were prepared by mixing 25% recycled HDPE pellets with 75% pristine HDPE pellets by weight. All test materials were prepared in the form of 3D printing filament using a lab-scale single screw extruder (Composer 350, 3Devo). The extruder contains four heating zones and one rotational screw at the center. The temperature for each heating zone ranged between 190 and 205°C, while the extrusion speed of the extruder varied between 2 and 2.7 rpm depending on the thickness of the filament. A higher speed resulted in thicker filaments, whereas a lower speed led to thinner filaments. After the parametric studies, the optimum range of temperatures and extrusion speed was found. The parameters used in this study are listed in Table 1. In addition.

For evaluation of the surface morphology and quality of extruded filaments, scanning electron microscopy (SEM) images were captured and shown in Fig. 3. Figs. 3(a) and 3(b) present the quality of filaments within and outside the optimum range. The filament produced outside the range has an oval shape that is not applicable for 3D printing where as the one produced within the range shows relatively uniform shape. Figs. 3(c) and 3(d) show an image of pristine and recycled HDPE, respectively, at a magnification level of 50x. The images revealed that pristine HDPE produces much smoother and better-quality of filaments than recycled HDPE. It should be noted that recycled HDPE used in this study was obtained from various sources such as water bottles and milk jugs. Therefore, it might include unidentified impurities in the pellets supplied.

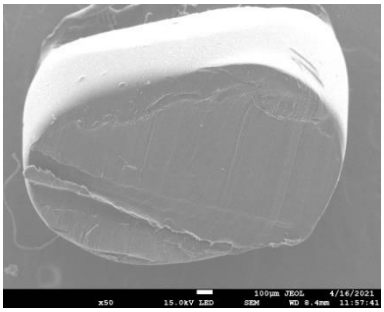
(a) Filament outside the optimum range

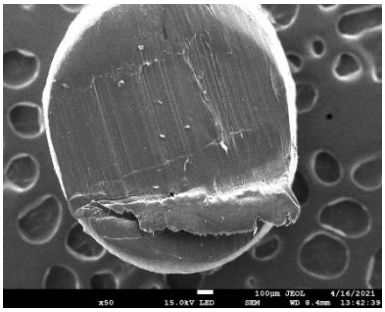
(b) Filament within the optimum range

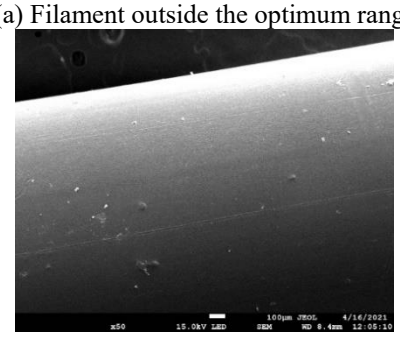
(c) Pristine HDPE

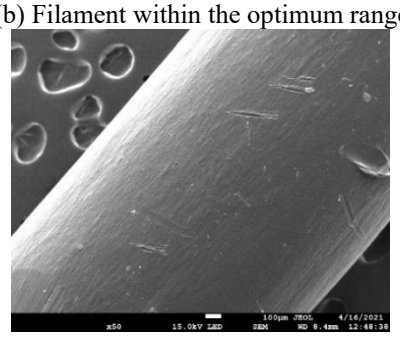
(d) Recycled HDPE

Fig. 3 SEM images of filaments manufactured by a single-screw extruder

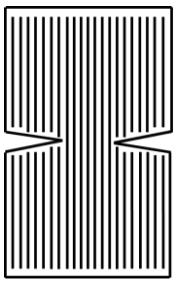

Fig. 4 3D printing pattern used for DENT specimens

Table 2 3D printing parameters

Parameters	Value
Nozzle temperature	245- 270°C
Build plate temperature	Room temperature, 22°C
Layer height	0.25 mm
Height of the first layer	0.28 mm
Line width	0.4 mm
Number of layers	4
Infill density (% Filled)	100%
Filling pattern	Linear lines
Filling angle	0°
Printing speed	20 – 25 mm/s
Build plate	Silicone rubber
Build plate condition	Adhesive liquid applied

3.2 Test specimen preparation

The double-edge notched tensile (DENT) specimens with a height of 150 mm, a width of 40 mm, and a thickness of 1 mm were prepared for the EWF concept test. The ligament length of the produced specimens varied from 5 to 12 mm to fulfill the plane-stress condition, as indicated in Eq. (4). All test specimens were fabricated by a commercially available 3D printer (Method X, Makerbot) employing the FDM technique. The specimens were printed using a 0.8 mm nozzle (LabsGen2, Makerbot) and a printing speed of 20 to 25 mm/s with a filling degree of 100% and a linear filling pattern at an angle of 0° to the longitudinal axis, as shown in Fig. 4. To increase the adhesion between molten plastic and a build plate, black silicone rubber with adhesive spray was used for the build plate material. Other parameters, such as nozzle temperature and layer structures for 3D printing, are listed in Table 2.

4. Results and discussion

4.1 Optimization of printing parameters

In order to fabricate high-quality specimens in 3D printing, the printing specimen must adhere to the build plate until the competition of the printing process. 3D printing of HDPE employing the FDM technique is challenging because of its high crystallinity. Crystallization induces high shrinkage of HDPE during the cooling process. It results in the warping of a specimen and detaching it from a build plate when it cools. Parametric studies to find the optimal printing condition for HDPE blends were therefore conducted. To prevent specimens from warping and maintain sufficient adhesive contact with a print bed, seven different print bed materials, including HDPE, ethylene propylene diene monomer (EPDM) rubber, polystyrene, neoprene rubber, styrene-butadiene rubber (SBR), natural rubber, and duct tape were tested. However, only two materials: HDPE and SBR were successful to achieve appropriate adhesion in our preliminary studies. Thus, this study used those two print bed materials.

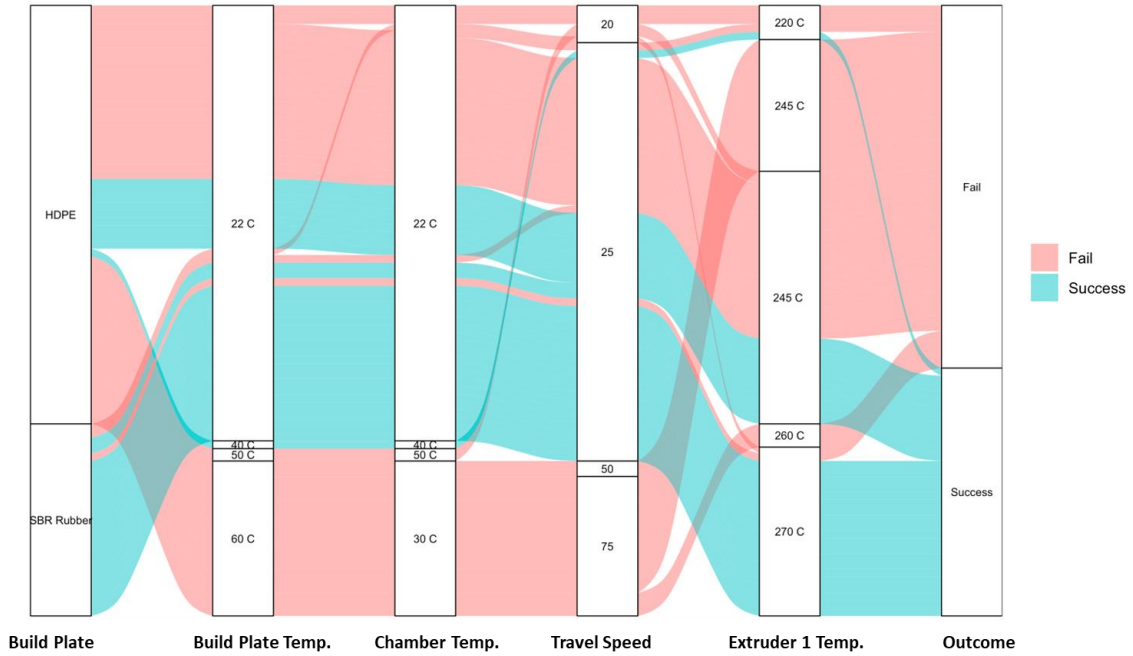

Fig. 5 Flow map displaying the optimized parameter

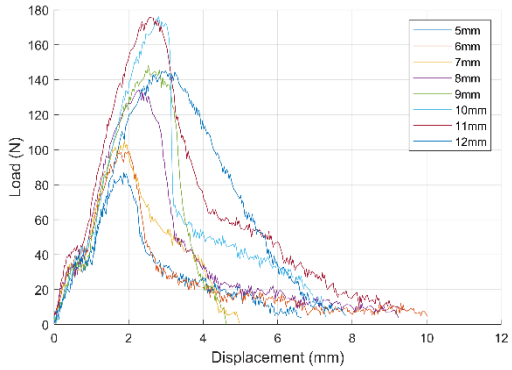

(a) Load-displacement curves with different ligament lengths

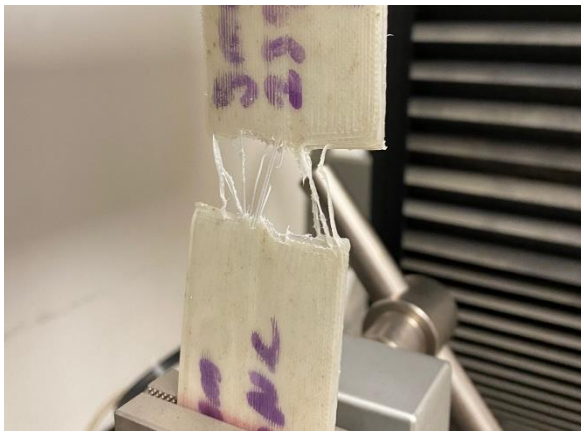

(b) Separation and deformation of layers after the failure

Fig. 6 DENT test results

Various parameters including build plate temperature, printer chamber temperature, nozzle travel speed, nozzle temperature as well as print bed materials were tested to find the optimal parameters. Fig. 5 displays the results of the parametric studies conducted to find the optimal conditions. The five parameters selected were represented by rectangles, and arcs were used for representing their links. The arcs green-colored lead to successful outcomes whereas the arcs red-colored lead to failure. For a HDPE print bed material, the combination of room temperature of the build plate and chamber, 25 mm/s of travel speed, and 245°C of extruder temperature resulted in the successful fabrication of specimens.

Other combinations resulted in ill-formed specimens, warping, or detaching. For SBR, most optimal conditions were similar to HDPE except for the extruder temperature. SBR required a higher extruder temperature (270°C) to produce sufficient adhesive contact. Temperatures below 270°C failed to generate appropriate adhesion. The results suggest that increasing temperatures of either a build plate or chamber had minimal effect on the fabrication of the specimens. Also, different build plate materials may require different extruder temperature conditions. It should be noted that the optimal parameters and printing conditions found in this study may be limited to the specific materials tested in this research. Our test materials include recycled HDPE obtained from various sources. The parameters can be varied with materials and printing conditions. For example, Schirmeister et al. (Schirmeister *et al.* 2019) reported different parameters for HDPE. They successfully manufactured HDPE specimens at a higher build plate temperature than that used in this study.

4.2 EWF test results

EWF tests were conducted on specimens with different

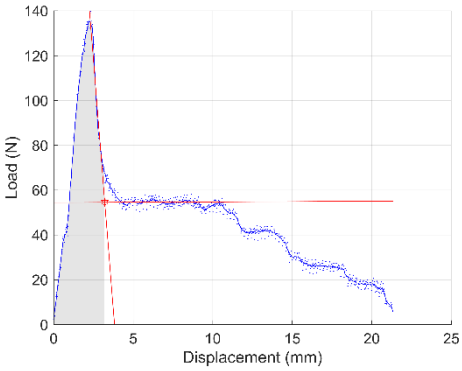

(a) Energy partitioning for 11 mm-ligament specimen

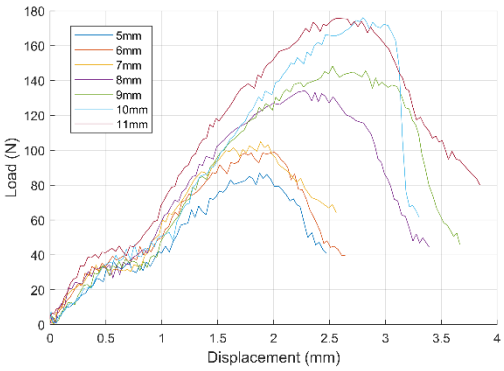

(b) Load-displacement curves after partitioning

Fig. 7 Energy partitioning approach and reconstructed load-displacement curves

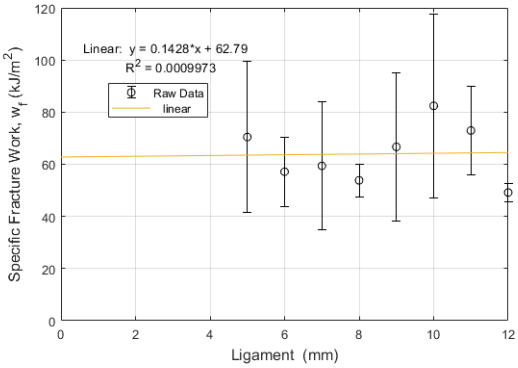

(a) Traditional EWF approach

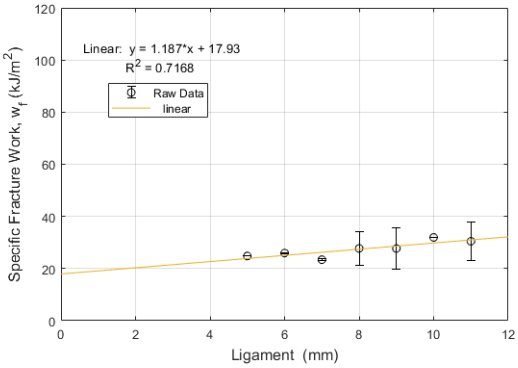

(b) New energy partitioning approach

Fig. 8 Specific work of fracture as a function of ligament length

ligament lengths ranging from 5 mm to 12 mm to ensure failure in the plane-stress condition. The tests subsequently generated a set of load-displacement curves, as shown in Fig. 6(a). The results show that the recorded load-displacement curves failed to satisfy self-similarity with different ligament lengths, which is one of the criteria for validating the EWF concept. Self-similarity offers the validity of tested specimens confirming that all specimens experience the identical failure mechanism. The random shape of the curves in Fig. 3(a) is mainly due to the intrinsic limit of the 3D printing process that produces an anisotropic layer-by-layer structure. In theory, the total energy defined by the area under the load-displacement curve must express the energy required to create a new fracture surface. However, it was observed that a part of the energy was consumed for the separation of specimen layers and deformation of the individual string rather than the formation of the crack, resulting in the random shape of the curve after load drop (see Fig. 6(b)). This energy should be excluded from the total fracture energy because it has nothing to do with the total fracture energy consumed by the fracture process. Therefore, the traditional EWF approach using the entire load-displacement curve is not applicable and should be modified for this specific type of specimen.

This study proposed a new energy partitioning method that separates fracture energy from the total work that includes unnecessary energies. This work-partitioning scheme is shown in Fig. 7(a), which is actual test data obtained from the 11mm-ligament specimen. A crack initiates when the load reached the peak. Once the crack propagates, the load drops at a nearly constant rate. However, a sudden change in the rate was observed shortly after the end of the constant load-dropping rate, as shown in Fig. 7(a). At this point, the separation of 3D printed layers takes place. Further increase in the displacement led to the tensile deformation of individual layers, as shown in Fig. 6(b). It may be arguable to identify the partitioning point because the transition locates in a nonlinear curve between two mechanisms. This study used the location where two linear trend lines intersect each other. Since each line reflects a different failure mechanism, the transition could be assumed to be the same as the intersection. The red dot in Fig. 7(a) shows the location of the partitioning point. Fig. 7(b) exhibits the reconstructed load-displacement curves after the partitioning. Each curve shows a nearly identical shape that satisfies the self-similarity of the EWF concept. This result reflects that the part before the partitioning point relates to the failure mechanism whereas the rest of the part does not contribute to the failure.

According to the EWF concept, values of the specific work of fracture (w_f) for each ligament were determined by the total area under the load-displacement curve and are plotted with respect to ligament length (Fig. 8). The specific

EWF value was subsequently obtained by extrapolating that separates fracture energy from the total work that includes unnecessary energies. This work-partitioning scheme is shown in Fig. 7(a), which is actual test data obtained from the 11mm-ligament specimen. A crack initiates when the load reached the peak. Once the crack propagates, the load drops at a nearly constant rate. However, a sudden change in the rate was observed shortly after the end of the constant load-dropping rate, as shown in Fig. 7(a). At this point, the separation of 3D printed layers takes place. Further increase in the displacement led to the tensile deformation of individual layers, as shown in Fig. 6(b). It may be arguable to identify the partitioning point because the transition locates in a nonlinear curve between two mechanisms. This study used the location where two linear trend lines intersect each other. Since each line reflects a different failure mechanism, the transition could be assumed to be the same as the intersection. The red dot in Fig. 7(a) shows the location of the partitioning point. Fig. 7(b) exhibits the reconstructed load-displacement curves after the partitioning. Each curve shows a nearly identical shape that satisfies the self-similarity of the EWF concept. This result reflects that the part before the partitioning point relates to the failure mechanism whereas the rest of the part does not contribute to the failure.

According to the EWF concept, values of the specific work of fracture (w_f) for each ligament were determined by the total area under the load-displacement curve and are plotted with respect to ligament length (Fig. 8). The specific EWF value was subsequently obtained by extrapolating values of (w_f) to zero ligament length. The obtained specific EWF value based on the conventional total energy approach is 62.8 kJ/m^2. However, the data points are scattered and inconsistent, resulting in a low correlation coefficient (R^2) of nearly 0 (Fig. 8(a)). Values of (w_f) calculated based on the energy partitioning method are also plotted in Fig. 8b. The data points become more consistent and provide a relatively higher R^2 value of 0.72. The specific EWF value obtained by the new approach is now 17.9 kJ/m^2. It has been reported that the fracture toughness of pristine HDPE pipe typically ranges from 35 to 138 kJ/m^2 (Mai and Cotterell 1986, Mai *et al.* 1987, Mai and Powell 1991) which is greater than our value. It should be noted that our test materials are recycled HDPE blends and 3D printed which should reduce the fracture toughness of HDPE. Therefore, we believe that the proposed energy partitioning method can be used to evaluate specific EWF values for 3D-printed HDPE blends.

Similar energy partitioning approaches have been proposed and used for the analysis of the EWF test. Karger-Kocsis *et al.* (Mouzakis *et al.* 2000, Karger-Kocsis and Ferrer-Balas 2001) proposed a partitioning approach to separate fracture energy for yielding from energy for necking. Those energies were determined by the area under the load-displacement curve before and after the point of the maximum load. Kwon and Jar (2007) also proposed an energy partitioning approach to extrapolate the plane-strain fracture energy from the total work. They identified the partitioning point based on the change in load-drop rate in a load-displacement curve. The novelty of our approach is to determine the pure fracture energy from the total energy that contains energies not related to fracture behavior while other approaches separate energy within the already defined fracture energy.

5. Conclusions

Recycled HDPE blends fabricated by the FDM 3D printing technique were tested to determine their fracture toughness. The fracture toughness was evaluated by the EWF concept. The results suggest that the traditional EWF approach does not apply to FDM 3D-printed specimens due to their intrinsic layer-by-layer structure. The traditional EWF approach utilizes an entire load-displacement curve of a failed specimen to compute the total fracture work. The approach assumes that the total work contributes to the formation and creation of new crack surfaces. Furthermore, all test specimens must exhibit an identical failure mechanism that can be verified by the self-similarity of load-displacement curves. This assumption may be only true for isotropically structured specimens. The FDM 3D printing technique produces an object that is anisotropic and has an intrinsic layer-by-layer structure. Because the bonding between layers might be relatively weaker than the intact material body, separation between layers and deformation of individual strings also occur during the testing. These energies are not related to crack formation but are still included in the load-displacement response, resulting in inconsistencies of load-displacement curves among test specimens. To overcome those limitations, this paper proposed a new energy partitioning approach. Combining experimental observations with post-analysis of load-displacement responses, it was found that those energies for separation and deformation could be distinguished after the constant rate of load drop. The new approach identified the energy partitioning location based on the change in load drop rate, and therefore successfully excluded the energies. This paper compared the results from both the traditional and new approaches and reported that the new energy partitioning approach provided more consistent results with a much higher correlation coefficient. In conclusion, the proposed new energy partitioning method allows us to apply the EWF concept for anisotropic 3D printed objects.

Acknowledgments

This research has been supported by a grant from the U.S. Environmental Protection Agency's (EPA) People, Prosperity and the Planet (P3) Student Design Competition program. The views expressed in this paper are solely those of the authors and do not necessarily reflect those of the Agency. EPA does not endorse any products or commercial services mentioned in this publication. The authors also gratefully acknowledge the Marshall University Molecular and Biological Imaging Center for the SEM part of the work, and we thank Michael L. Norton and David Neff for their training and assistance.

References

American Chemistry Council (2022), *PIPS Resin Sales and Production CY Figures, 2021 vs 2020* American Chemistry Council

Aurrekoetxea, J., Sarrionandia, M.A., Urrutibeascoa, I. and Maspoch, M.L. (2001), "Effects of recycling on the microstructure and the mechanical properties of isotactic polypropylene", *J. Mater. Sci.*, **36**(11), 2607-2613. https://doi.org/10.1023/A:1017983907260.

Broberg, K. (1968), "Critical review of some theories in fracture mechanics", *Int. J. Fract. Mech.*, **4**(1), 11-19. https://doi.org/10.1007/BF00189139.

Broberg, K.B. (1971), "Crack-growth criteria and non-linear fracture mechanics", *J. Mech. Phys. Solids*, **19**(6), 407-418. https://doi.org/10.1016/0022-5096(71)90008-1.

Broberg, K.B. (1975), "On stable crack growth", *J. Mech. Phys. Solids*. **23**(3), 215-237. https://doi.org/10.1016/0022-5096(75)90017-4.

Chan, W.Y.F. and Williams, J.G. (1994), "Determination of the fracture toughness of polymeric films by the essential work method", *Polymer*, **35**(8), 1666-1672. https://doi.org/10.1016/0032-3861(94)90840-0.

Ching, E.C.Y., Poon, W.K.Y., Li, R.K.Y. and Mai, Y.W. (2000), "Effect of strain rate on the fracture toughness of some ductile polymers using the essential work of fracture (EWF) approach", *Polymer Eng. Sci.*, **40**(12), 2558-2568. https://doi.org/10.1002/pen.11386.

Cotterell, B. and Reddel, J. (1977), "The essential work of plane stress ductile fracture", *Int. J. Fracture*. **13**(3), 267-277. https://doi.org/10.1007/BF00040143.

Ghadr, S., Mirsalehi, S. and Assadi Langroudi, A. (2019), "Compacted expansive elastic silt and tyre powder waste", *Geomech. Eng.*, **18**(5), 535-543. https://doi.org/10.12989/gae.2019.18.5.535.

Gudadhe, A., Bachhar, N., Kumar, A., Andrade, P. and Kumaraswamy, G. (2019), "Three-Dimensional Printing with Waste High-Density Polyethylene", *ACS Appl. Polymer Mater.*, **1**(11), 3157-3164. https://doi.org/10.1021/acsapm.9b00813.

Karger-Kocsis, J. and Ferrer-Balas, D. (2001), "On the plane-strain essential work of fracture of polymer sheets", *Polymer Bull.*. **46**(6), 507-512. https://doi.org/10.1007/s002890170039.

Komurlu, E., Kesimal, A. and Demir, S. (2016), "Experimental and numerical analyses on determination of indirect (splitting) tensile strength of cemented paste backfill materials under different loading apparatus", *Geomech. Eng.*, **10**(6), 775-791. http://dx.doi.org/10.12989/gae.2016.10.6.775.

Kwon, H.J. and Jar, P.Y.B. (2007), "New energy partitioning approach to the measurement of plane-strain fracture toughness of high-density polyethylene based on the concept of essential work of fracture", *Eng. Fract. Mech.*, **74**(16), 2471-2480. https://doi.org/10.1016/j.engfracmech.2006.12.028.

La Mantia, F.P. (1999), "Mechanical properties of recycled polymers", *Macromol. Symposia*, **147**(1), 167-172. https://doi.org/10.1002/masy.19991470116.

Levita, G., Parisi, L. and Marchetti, A. (1994), "The work of fracture in semiductile polymers", *J. Mater. Sci.*, **29**(17), 4545-4553. https://doi.org/10.1007/BF00376277.

Liu, H., Yang, G., Wang, H. and Xiong, B. (2017), "A large-scale test of reinforced soil railway embankment with soilbag facing under dynamic loading", *Geomech. Eng.*, **12**(4), 579-593. https://doi.org/10.12989/gae.2017.12.4.579.

Mai, Y.-W. and Cotterell, B. (1986), "On the essential work of ductile fracture in polymers", *Int. J. Fracture*, **32**(2), 105-125. https://doi.org/10.1007/BF00019787.

Mai, Y.W., Cotterell, B., Horlyck, R. and Vigna, G. (1987), "The essential work of plane stress ductile fracture of linear polyethylenes", *Polymer Eng. Sci.*, **27**(11), 804-809. https://doi.org/10.1002/pen.760271106.

Mai, Y.W. and Pilko, K.M. (1979), "The essential work of plane stress ductile fracture of a strain-aged steel", *J. Mater. Sci.*, **14**(2), 386-394. https://doi.org/10.1007/BF00589830.

Mai, Y.W. and Powell, P. (1991), "Essential work of fracture and j-integral measurements for ductile polymers", *J. Polymer Sci. Part B: Polymer Phys.*, **29**(7), 785-793. https://doi.org/10.1002/polb.1991.090290702.

Maruvanchery, V. and Kim, E. (2019), "Effects of water on rock fracture properties: Studies of mode I fracture toughness, crack propagation velocity, and consumed energy in calcite-cemented sandstone", *Geomech. Eng.*, **17**(1), 57-67. https://doi.org/10.12989/gae.2019.17.1.057.

Mouzakis, D., Karger-Kocsis, J. and Moskala, E. (2000), "Interrelation between energy partitioned work of fracture parameters and the crack tip opening displacement in amorphous polyester films", *J. Mater. Sci. Lett.*, **19**(18), 1615-1619. https://doi.org/10.1023/A:1006797522901.

Na, S., Nguyen, L., Spatari, S. and Hsuan, G.Y. (2016), "Evaluating the effect of nanoclay and recycled HDPE on stress cracking in HDPE using j-integral approach", *ANTEC. Society of Plastic Engineers, Indianapolis*.

Na, S., Nguyen, L., Spatari, S. and Hsuan, Y.G. (2018), "Effects of recycled HDPE and nanoclay on stress cracking of HDPE by correlating Jc with slow crack growth", *Polymer Eng. Sci.,* **58**(9), 1471-1478. https://doi.org/10.1002/pen.24691.

Na, S., Spatari, S. and Hsuan, Y.G. (2015), "Fracture characterization of pristine/post-consumer HDPE blends using the essential work of fracture (EWF) concept and extended finite element method (XFEM)", *Eng. Fract. Mech.*, **139**, 1-17. https://doi.org/10.1016/j.engfracmech.2015.02.026.

Na, S., Spatari, S. and Hsuan, Y.G. (2016), "Fracture characterization of recycled high density polyethylene/nanoclay composites using the essential work of fracture concept", *Polymer Eng. Sci.*, **56**(2), 222-232. https://doi.org/10.1002/pen.24250.

Paton, C.A. and Hashemi, S. (1992), "Plane-stress essential work of ductile fracture for polycarbonate", *J. Mater. Sci.*, **27**(9), 2279-2290. https://doi.org/10.1007/BF01105033.

Pattanakul, C., Selke, S., Lai, C. and Miltz, J. (1991), "Properties of recycled high density polyethylene from milk bottles", *J. Appl. Polymer Sci.*, **43**(11), 2147-2150. https://doi.org/10.1002/app.1991.070431122.

Schirmeister, C.G., Hees, T., Licht, E.H. and Mülhaupt, R. (2019), "3D printing of high density polyethylene by fused filament fabrication", *Additive Manufact.*, **28**, 152-159. https://doi.org/10.1016/j.addma.2019.05.003.

Terzi, N.U., Erenson, C. and Selcuk, M.E. (2015), "Geotechnical properties of tire-sand mixtures as backfill material for buried pipe installations", *Geomech. Eng.*, **9**(4), 447-464. https://doi.org/10.12989/gae.2015.9.4.447.

Usman, A., Sutanto, M.H., Napiah, M., Zoorob, S.E. and Al-Sabaeei, A.M. (2021), "Optimization of irradiated waste polyethylene terephthalate modified asphalt pavement using response surface methodology", *Geomech. Eng.*, **26**(6), 513-527. https://doi.org/10.12989/gae.2021.26.6.513.

Williams, J.G. and Rink, M. (2007), "The standardisation of the EWF test", *Eng. Fract. Mech.*, **74**(7), 1009-1017. https://doi.org/10.1016/j.engfracmech.2006.12.017.

Wu, J. and Mai, Y.-W. (1996), "The essential fracture work concept for toughness measurement of ductile polymers", *Polymer Eng. Sci.*, **36**(18), 2275-2288. https://doi.org/10.1002/pen.10626.

Wu, J., Mai, Y.W. and Cotterell, B. (1993), "Fracture toughness and fracture mechanisms of PBT/PC/IM blend", *J. Mater. Sci.*, **28**(12), 3373-3384. https://doi.org/10.1007/BF00354261